

# High Capacity Hydrogen Storage in Ca Decorated Graphyne: A First-Principles Study

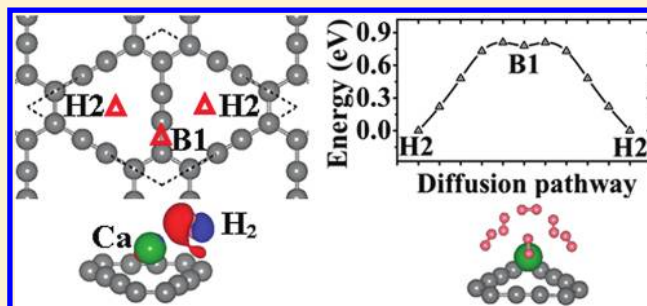
Chong Li,<sup>†</sup> Jingbo Li,<sup>\*,†,‡</sup> Fengmin Wu,<sup>‡</sup> Shu-Shen Li,<sup>†</sup> Jian-Bai Xia,<sup>†</sup> and Lin-Wang Wang<sup>\*,§</sup>

<sup>†</sup>State Key Laboratory for Superlattices and Microstructures, Institute of Semiconductors, Chinese Academy of Sciences, P.O. Box 912, Beijing 100083, China

<sup>‡</sup>Zhejiang Normal University, Jinhua 321004, Zhejiang Province, China

<sup>§</sup>Material Science Division, Lawrence Berkeley National Laboratory, Berkeley, California 94720, United States

**ABSTRACT:** Ca decorated carbon allotropes have a potential for high density hydrogen storage, except that the Ca–graphene and Ca–fullerenes binding is not strong enough to prevent the formation of a Ca cluster. Using first-principles calculations, we show that Ca can bind strongly to s–p and s–p<sup>2</sup> bonded graphyne without the formation of a Ca cluster. This enhanced binding energy is due to the additional in-plane  $\pi$  states which do not exist in the s–p<sup>2</sup> bonded graphene and fullerenes. The H<sub>2</sub> binding to the Ca–graphyne system is similar to the Ca–fullerenes system with a maximum of six H<sub>2</sub> molecules per Ca atom and a 0.2 eV per H<sub>2</sub> binding energy which is optimal as hydrogen storage materials. With two Ca atoms per unit cell, this leads to 9.6 wt % hydrogen storage capacity in theory.



## INTRODUCTION

Hydrogen is considered to be an ideal clean energy source that could one day replace fossil fuels to combat global warming.<sup>1</sup> One of the biggest challenges to reach that goal is the high density hydrogen storage. To perform reversibly hydrogen charging cycles at ambient conditions for automobile onboard applications, a desired storage system should have high gravimetric density (>9 wt %) by the year 2015 and a binding energy of hydrogen molecule at 0.2–0.4 eV.<sup>2,3</sup> One promising approach is to use decorated fullerene like buckyball, carbon nanotube, or graphene.<sup>4</sup> The decorating atoms can be transition metals (TM),<sup>5–7</sup> alkaline metals (AM),<sup>8</sup> or alkaline earth metals (AEM).<sup>9–13</sup> Each TM or AEM (Ca, Sr) atom can bind up to six hydrogen molecules<sup>6,9,11</sup> in the right energy range due to the coordination bonding between the empty d states in the metal atom and the occupied s states in hydrogen molecules. The six H<sub>2</sub> per metal atom binding will provide sufficient weight density especially for light metals like Ca. This makes the Ca atom one of the most promising decorating metal atoms.<sup>9,10</sup> One major challenge, however, is to find the right framework to stably hold the Ca as individual atoms without clustering. For the case of s–p<sup>2</sup> bond fullerene/graphene decoration, this depends on the binding energy between the Ca atom and the carbon atoms. Such binding comes from the interaction of the Ca atom with the fullerene  $\pi/\pi^*$  states (where  $\pi$  is the occupied bonding  $\pi$  state and  $\pi^*$  is the unoccupied antibonding  $\pi^*$  state), where the Ca atom donates the 4s electrons to the empty  $\pi^*$  states (which are heavily hybridized with the empty Ca 3d states and hence provide some electron back-donation). Unfortunately, due to the perpendicular orientation of the  $\pi/\pi^*$  states to the carbon plane, and

the spacing between different  $\pi/\pi^*$  states, there is not a single spatial site where the Ca atom can fully engage with multiple  $\pi/\pi^*$  bond interactions. As a result, the maximum Ca binding energy (which happens at a site above the center of the hexagonal carbon ring) is relatively small at about 0.9 eV,<sup>9–11</sup> which is less than the Ca–Ca cluster cohesive energy of 1.84 eV. This makes the Ca fullerene binding unstable, and the Ca cluster will form in practice.<sup>14</sup> Incorporating impurity in the carbon nanotube is proposed to enhance the Ca–carbon binding, but the impurity concentration is limited.<sup>11</sup>

In this article, through ab initio calculation, we show that the highly anticipated graphyne can be used as an ideal framework material to hold the Ca atoms. The additional in-plane p<sub>x</sub>–p<sub>y</sub> orientated  $\pi/\pi^*$  states and the proper size of the ring formed by the acetylenic (–C≡C–) bonds make the Ca–graphyne binding very strong at 2.76 eV, which is bigger than the Ca–Ca cohesive energy of 1.84 eV, thus making the structure highly stable. We find that the 9.6 wt % of hydrogen storage can be reached by binding 6H<sub>2</sub> molecules at each Ca atom with an average binding energy of ~0.2 eV. This will place this system as one of the most promising hydrogen storage materials. Although the theoretically predicted graphyne<sup>15–18</sup> has yet to be synthesized, recently a very similar graphdiyne film has been experimentally synthesized over a copper substrate.<sup>19</sup> Graphdiyne has two –C≡C– bonds instead of one at each link between two carbon hexagonal rings, and its formation energy is slightly

**Received:** August 31, 2011

**Revised:** October 10, 2011

**Published:** October 14, 2011

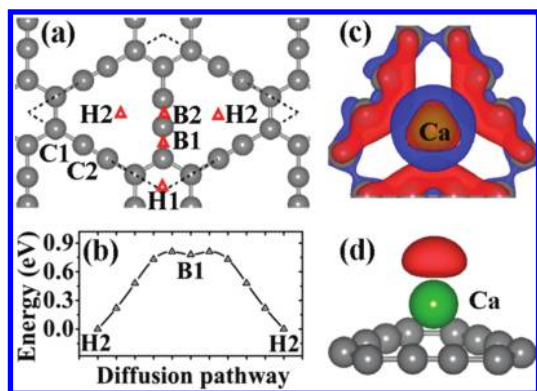


**Figure 1.** Schematics of (a) the structure of graphyne and the four adsorption sites are shown by red empty triangles. C  $s-p^2$  and  $s-p$  hybridization are denoted by C1 and C2, respectively. The unit cell is indicated by dashed lines. (b) Diffusion pathway for a single Ca atom on graphyne. (c) Calculated charge density differences of the Ca decorated graphyne system ( $\rho_{\text{sheet+metal}} - \rho_{\text{sheet}} - \rho_{\text{metal}}$ ); the red color and blue color represent charge accumulation and depletion, respectively. (d) Spin polarized charge density ( $\rho_{\uparrow} - \rho_{\downarrow}$ ). In (c) and (d), the isosurface charge density is taken to be  $0.0038 \text{ e}/\text{\AA}^3$ .

(0.17 eV) less (less stable) than graphyne.<sup>16</sup> Thus, it looks like it is only a matter of time before the more stable and simpler graphyne will be synthesized in the future. Our work will put a further urgency on the experimental synthesis of graphyne.

## CALCULATION METHOD

The calculations are carried out using the Vienna ab initio simulation package (VASP)<sup>20</sup> with the projector-augmented-wave (PAW) method.<sup>21</sup> We select the spin-polarized generalized gradient approximation (GGA) with Perdew, Burke, and Ernzerhof (PBE)<sup>22,23</sup> for exchange-correlation energy. Here the effect of van der Waals (vdW) interactions is included explicitly by using the empirical correction scheme of Grimme (DFT+D2),<sup>24</sup> as implemented by Bucko et al.<sup>25</sup> for periodic systems. Standard values of the dispersion coefficients  $C_6$  (0.14, 1.75, and  $10.80 \text{ J nm}^6 \text{ mol}^{-1}$ , for H, C, and Ca, respectively), vdW radii (1.001, 1.452, and  $1.474 \text{ \AA}$ ), cutoff radius for pair interactions ( $30.0 \text{ \AA}$ ), PBE global scaling factor  $S_6$  (0.75), and damping factor  $d$  (20.0) have been used. For comparison, local density approximation (LDA)<sup>26</sup> is also used since it is often employed to describe the carbon bonding and hydrogen carbon interactions.<sup>10,12,27</sup> A 500 eV cutoff energy is chosen for the plane-wave basis. The  $k$ -point meshes for Brillouin zone sampling are constructed with a Monkhorst–Pack scheme,<sup>28</sup> and  $8 \times 8 \times 1$   $k$ -point meshes are used for structural relaxations until the Hellmann–Feynman force is less than  $0.02 \text{ eV}/\text{\AA}$ .

## RESULTS AND DISCUSSION

We first studied the case of a single metal Ca adsorption on graphyne. Figure 1(a) shows schematically the structures of graphyne. The graphyne has been theoretically predicted to be a stable structure (although with a formation energy 1 eV per atom smaller than that of graphite) with a 0.9 eV band gap.<sup>15–18</sup> Our calculated lattice constant of graphyne is  $6.88 \text{ \AA}$ , in line with the previous results.<sup>16</sup> We use a  $(1 \times 1)$  graphyne unit cell to model the adsorption systems, and a  $16 \text{ \AA}$  vacuum layer is added to ensure the adjacent layers are decoupled. Four local stable sites

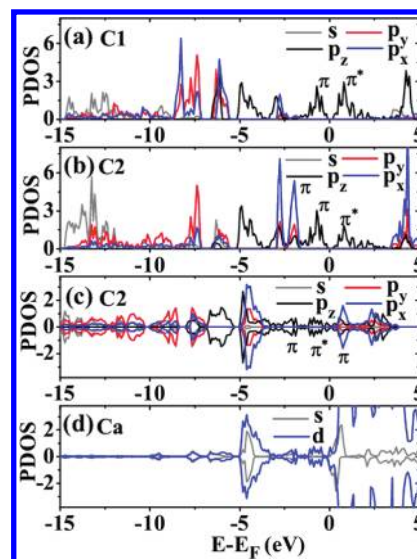


**Figure 2.** Calculated partial density of states (PDOS) for (a) C1 and (b) C2 atoms of pure graphyne, respectively, and (c) C2 and (d) Ca atoms of Ca decorated graphyne.

for Ca atom adsorption are shown in Figure 1(a), namely, H1, H2, B1, and B2 sites. We find that not H1 but H2 is the most stable adsorption site, and the calculated binding energy of one Ca in one unit cell (which has two acetylenic rings as shown in Figure 1(a)) is 2.76 eV (LDA: 3.29 eV), which is much larger than the Ca metal cohesive energy of 1.84 eV, indicating that Ca atoms will be dispersed evenly on graphyne, instead of forming metal clusters. The strong Ca–carbon bonding is attributed to the additional  $p_x-p_y/\pi/\pi^*$  states existing in the  $-C\equiv C-$  bonds. Unlike the  $s-p^2$  hybridization in graphene, where only out-of-plane  $p_z/\pi/\pi^*$  states exist (here  $z$  is the direction perpendicular to the carbon plane), here there are also in-plane  $p_x-p_y/\pi/\pi^*$  states. This enables the  $\pi/\pi^*$  states to rotate toward any direction perpendicular to the line of  $-C\equiv C-$ , thus making it possible for the  $\pi/\pi^*$  states from the three  $-C\equiv C-$  bonds at a given acetylenic ring to all point toward the Ca atom. Moreover, we also find that the B1 site is slightly more stable than the B2 site, indicating that the Ca atom binds stronger to  $-C-C-$  than  $-C\equiv C-$  bonds in the  $z$  direction. The minimum energy position of Ca at the H2 point is  $1.42 \text{ \AA}$  away from the carbon plane. Two Ca atoms can simultaneously decorate a single unit cell, thus filling both acetylenic rings, but they prefer to be at the opposite sides of the carbon plane and to be shifted slightly from the symmetric H2 points to avoid Coulomb interaction between them. The binding energy in that case is 2.51 eV (LDA: 3.00 eV) per Ca, and the Ca–carbon plane distance is  $1.45 \text{ \AA}$ .

To further check the stability of the Ca decorated graphyne system, we also use the ab initio molecular dynamics (MD) simulations for the case of one Ca in one unit cell. In the simulations, the temperature gradually increases from 0 to 900 K in 300 time steps, and the time step is 3 fs, which is deliberately large to possibly make the structure unstable. We find that the Ca decorated graphyne does not undergo an obvious deformation even at the temperature of 900 K, and the adsorbed Ca atom remains at the H2 site and does not diffuse to the nearest neighboring H2 site on graphyne. In contrast, for the case of Ca on graphene, the Ca atom can diffuse when the temperature is

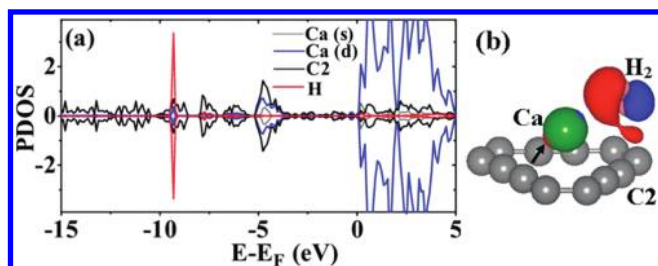


**Figure 3.** Calculated (a) PDOS and (b) charge density differences for  $\text{H}_2$  adsorbed on Ca decorated graphyne, respectively. The gained electrons of the Ca atom are indicated by a black arrow.

over 300 K<sup>10</sup> under the same ab initio MD simulation with the same number of MD steps.

The Ca diffusion barrier is calculated using the “Nudged Elastic Band” (NEB) method.<sup>29</sup> The minimum barrier diffusion path happens naturally from H2 to B1 to H2, as shown in Figure 1(b). The diffusion barrier is 0.82 eV, which is much higher than the 0.15 eV barrier for Ca atom diffusion on graphene. Such a high diffusion barrier is ascribed to the strong Ca–carbon bonding and large “holes” of acetylenic rings in graphyne. This indicates that the Ca atoms will mostly be stable at the H2 sites at room temperature and also explains why there is no diffusion in our MD simulation.

We have also calculated the charge transfer between metal Ca and graphyne to illustrate the binding of the Ca atom to the carbon atoms in graphyne. Figure 1(c) shows the charge flow due to the Ca binding with graphyne. Overall, we can see that the electrons of metal Ca are transferred to graphyne. Meanwhile, electrons are also accumulated on top of the Ca atom. In the process of electrons transferring between Ca and graphyne, Ca becomes spin-polarized (see Figure 1(d)) and possesses a small localized magnetic moment ( $\sim 0.25\mu_B$ ). On the contrary, there is no spin-polarized phenomenon in the Ca decorated graphene.<sup>10</sup>

To further understand the charge transfer and delineate the contribution of different hybridization states, we plotted the partial density of states (PDOS) of both pristine and Ca decorated graphyne systems in Figure 2. The PDOS has been separated into the  $s-p^2$  (C1) binding carbon atom and  $s-p$  (C2) binding carbon atom (see also Figure 1(a)), as well as the carbon s, p and Ca s, d states. For the pristine graphyne, the states near the valence band maximum (VBM) and conduction band minimum (CBM) are bonding  $p_z \pi$  and antibonding  $p_z \pi^*$  states, respectively, contributing from both C1 and C2 atoms. However, for the C2 atoms (see Figure 2(b)), there are two additional highly localized bonding  $p_x + p_y, \pi$  states, around 2.5 eV below the Fermi energy. Note that the in-plane carbon  $p_x, p_y$  states can contribute to both the  $\sigma$  bond and  $\pi$  bond. The  $\sigma$  bond happens at 6 eV below the Fermi level, while the  $\pi$  bonds and  $\pi^*$  states happen within the energy window of  $[-5:5]$  eV. After Ca is adsorbed on graphyne, the energy of the C2  $p_x + p_y, \pi$  states dropped from  $-2$  eV to about  $-5$  eV, while a major part of the C2  $p_z \pi$  bond lowers its energy to about  $-7$  eV and part of the C2  $p_z \pi^*$  state becomes occupied. For the Ca atom, part of its 4s states becomes unoccupied, indicating the donation of its electrons to the C2 carbon, while part of its 3d states becomes occupied with the same energy as the C2  $p_x + p_y, \pi$  bond. This means strong hybridization between the Ca 3d state and the C2  $p_x + p_y, p_z \pi$  state and also means back-donation of the electron from the C2 atom to the Ca atom. The overall binding picture is quite similar

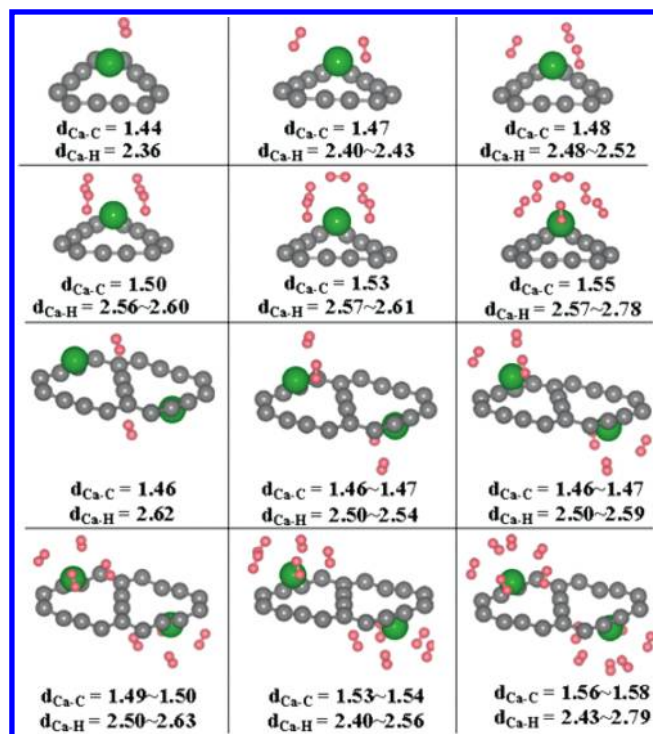


**Figure 4.** Schematics of adsorption sites of Ca on graphyne and  $\text{H}_2$  molecules binding to Ca atoms. Both single side and double sides of Ca decorated graphyne are shown. The distances between Ca atoms and the graphyne layer ( $d_{\text{Ca-C}}$ ) and between Ca atoms and  $\text{H}_2$  molecules ( $d_{\text{Ca-H}}$ ) are listed.

to the donation/back-donation mechanism introduced for the Ca–( $s-p^2$  carbon) system,<sup>9</sup> except that here there are  $s-p$  binding C2  $p_x + p_y, \pi/\pi^*$  bonds, in addition to the  $p_z$  bonds in the  $s-p^2$  system, and they hybridize heavily with the Ca 3d states. They are the prime reason why the Ca–graphyne binding is so much stronger than the Ca–( $s-p^2$  carbon) system binding. The Ca–graphyne system is also slightly spin polarized with the spin density coming from both the Ca 4s and 3d states (see Figure 2-(d)) and spatially localized above the Ca atom as shown in Figure 1(d).

On the basis of the above investigation of the stability of Ca decorated graphyne, now we study the interaction between this complex and  $\text{H}_2$  molecules. When one  $\text{H}_2$  molecule is adsorbed, the adsorbed  $\text{H}_2$  prefers to tilt toward the Ca atom, instead of parallel to it, and tends to locate at the nearby C2 atom, as shown in Figure 3(b). This lowest-energy configuration is found after testing many initial  $\text{H}_2$  positions followed by atom relaxations. Upon close inspection, we found that there is a weak hybridization between the occupied  $\text{H}_2 \sigma$  states ( $\sim 10$  eV below the Fermi energy) and the empty Ca 3d orbitals and also C2  $\sigma$  states (see Figure 3(a)). Thus, a weak coordination bond is formed. A similar hybridized interaction between  $\text{H}_2 \sigma$  states and Ca 3d orbitals also exists in  $\text{H}_2$  adsorbed on Ca decorated C nanotubes and graphene.<sup>10,11</sup> Surprisingly,  $\text{H}_2$  and Ca become nonspin-polarized upon adsorption of the  $\text{H}_2$  molecule. The charge density differences further clarify the hybridized interaction (also see Figure 3(b)), where the  $\text{H}_2$  molecule obviously occurs polarized, some electrons are accumulated between  $\text{H}_2$  and the C2 atom, and the Ca atom transfers some of its own electrons to the  $\text{H}_2$  molecule. At the same time, the Ca atom also gains a little



**Table 1.** Comparison of the Binding Energy  $E_b$  (eV) for  $H_2$  Molecules Binding to Single and Double Sides of Ca Decorated Graphyne by GGA+vdW and LDA

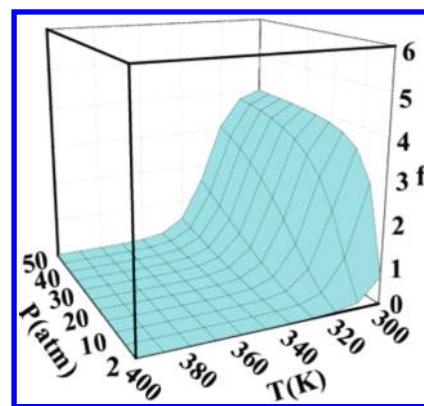
			1H <sub>2</sub>	2H <sub>2</sub>	3H <sub>2</sub>	4H <sub>2</sub>	5H <sub>2</sub>	6H <sub>2</sub>
$E_b$	1Ca	LDA	0.34	0.35	0.36	0.32	0.30	0.27
		GGA+vdW	0.23	0.26	0.27	0.24	0.22	0.19
	2Ca	LDA	0.25	0.29	0.31	0.32	0.30	0.27
		GGA+vdW	0.16	0.19	0.22	0.24	0.22	0.18

charge as a result of hybridization involving d-states. As a result, both the Ca atom and  $H_2$  molecule become polarized and interact on each other. Thus, the binding of  $H_2$  to Ca atoms originates from both its polarization caused by the electronic field produced by charged Ca and weak hybridization between  $H_2$  occupied  $\sigma$  states and empty Ca 3d orbitals.

Next, we investigated the possible number of  $H_2$  binding to Ca atoms. We have tested many different possible adsorption  $H_2$  configurations, based on both physical intuition and random initial positions, followed by atomic relaxations. The most stable configurations of adsorption with different numbers of  $H_2$  molecules on one Ca per unit cell and two Ca per unit cell cases are plotted in Figure 4. From Figure 4, we can see clearly that  $H_2$  molecules like to tilt away from the parallel position to the Ca atoms when the number of  $H_2$  is less than four. Note that the fifth  $H_2$  is parallel to the Ca atom for single side adsorption, while all five  $H_2$  molecules tilt from the parallel position for double side adsorption. Six  $H_2$  molecules can be effectively adsorbed on one Ca for both the cases of single side and double side Ca decorated graphyne, and the maximum  $d_{Ca-H}$  is 2.79 Å for the case of double side adsorption. On the whole, the distances between Ca atoms and graphyne ( $d_{Ca-C}$ ) and Ca atoms and  $H_2$  ( $d_{Ca-H}$ ) increase slightly as the number of  $H_2$  increases. For each configuration, the bond lengths of  $H_2$  molecules are in the range of 0.76–0.78 Å, only slightly larger than that of the isolated  $H_2$  molecule 0.76 Å. The molecular binding energies ( $E_b$ ) can be calculated as

$$E_b = -(E_{nH_2 + (metal + sheet)} - E_{(metal + sheet)} - nE_{H_2})/n \quad (1)$$

where  $E_{nH_2 + (metal + sheet)}$  and  $E_{(metal + sheet)}$  are the total energies of the Ca–graphyne complex with and without adsorbed  $nH_2$  molecules, respectively, and  $E_{H_2}$  is the energy of an isolated  $H_2$  molecule. The calculated  $E_b$  are summarized in Table 1. For one side adsorption, the  $E_b$  of one  $H_2$  adsorption is 0.23 eV, and it gradually increases as the adsorption number of  $H_2$  increases. The maximum  $E_b$  is reached when four  $H_2$  bind to one Ca atom. After that, the  $E_b$  decreases and becomes 0.19 eV for six  $H_2$  adsorption. For the case of both sides adsorption, the changing trend of  $E_b$  is very similar to the case of one side adsorption. To compare with the results of  $E_b$  calculated by GGA+vdW, we also use LDA to check the results and find that the resulting geometries are very close to the case of GGA+vdW calculations, and in general, the calculated  $E_b$  by LDA are higher by 0.08–0.10 eV than the case of GGA+vdW, as also seen in Table 1. The maximum binding number of  $H_2$  to each Ca atom still remains six, which is similar to Ca–C<sub>60</sub> and Ca–nanotube results.<sup>6,11</sup> Our  $H_2$  binding energy is in the range of 0.2–0.3 eV judged from both GGA+vdW and LDA results. Such binding energy is perfect for the practical hydrogen storage applications. For double side Ca decorations, the total number

**Figure 5.** Calculated occupation number ( $f$ ) of  $H_2$  molecules binding to double sides of Ca–graphyne as a function of temperature ( $T$ ) and pressure ( $P$ ) as calculated by the GGA+vdW method.**Table 2.** Comparison of the Thermodynamically Practical Usable Capacity  $G_{\text{prac}}$  (wt %) in Three Different Adsorption Systems, Namely, Ca–Graphyne, Ca–Carbyne,<sup>32</sup> and Ca–Graphene<sup>9</sup>

		$N_{\text{max}}$	$N_{\text{use}}/N_{\text{ads}} - N_{\text{des}}$	$G_{\text{max}}$ (wt %)	$G_{\text{prac}}$ (wt %)
GGA+vdW	Ca–graphyne	6	3.94/3.94–0.00	9.67	6.35
GGA	Ca–carbyne	6	3.97/3.98–0.01	8.16	5.59
LDA	Ca–graphyne	6	4.54/4.56–0.02	9.67	7.32
	Ca–graphene	4	3.84/4.00–0.00	8.33	7.97

of  $H_2$  binding to a unit cell is 12, which leads to a storage capacity of 9.6 wt %.

To get a more quantitative picture of  $H_2$  absorption at different temperature ( $T$ ) and pressure ( $P$ ), we will now estimate the thermodynamic properties of the system using some simple formulas. The averaged number of  $H_2$  binding at each Ca atom at equilibrium can be estimated following the simple formula given in ref 30

$$f = \frac{\sum_{l=0}^{N_{\text{max}}} l g_l e^{l(\mu - \varepsilon_l)/k_B T}}{\sum_{l=0}^{N_{\text{max}}} g_l e^{l(\mu - \varepsilon_l)/k_B T}} \quad (2)$$

where  $N_{\text{max}}$  is the maximum binding number of  $H_2$  molecules to each Ca atom;  $l$  is the binding number of  $H_2$ ;  $g_l$  is the configurational degeneracy for a given  $l$ ;  $k_B$  is the Boltzmann constant;  $-\varepsilon_l$  is the binding energy of  $H_2$  to Ca–graphyne (which is listed in Table 1); and  $\mu$  is the  $H_2$  gas phase chemical potential at given  $T$  and  $P$  (defined as without the zero temperature  $H_2$  energy). By using this formula, we have ignored the phonon contribution to the entropy. Furthermore, for simple estimation, we consider only one configuration as listed in Table 1 for each  $l$ . The  $H_2$  gas chemical potential  $\mu$  as a function of  $T$  and  $P$  is taken from the experimental values given in ref 30. Figure 5 shows the occupation number  $f$  of  $H_2$  molecules as a function of  $T$  and  $P$  for double side adsorption of  $H_2$  as calculated by the GGA+vdW method. The occupation number  $f$  is 3.94 at 30 atm and 25 °C, and  $f$  is almost zero at 3 atm and 100 °C. Here we provisionally choose 30 atm and 25 °C as the absorbing condition and 3 atm and

100 °C as the desorbing condition.<sup>30,31</sup> Table 2 lists the thermodynamically usable binding number ( $N_{\text{use}} = N_{\text{ads}} - N_{\text{des}}$ ) of H<sub>2</sub> to Ca–graphyne. We can see that the practical usable number  $N_{\text{use}}$  at adsorption condition is 3.94 per Ca atom, as calculated by GGA+vdW. This corresponds to a practical usable capacity  $G_{\text{prac}}$  of 6.35 wt %. The corresponding numbers for LDA results are 4.56 H<sub>2</sub> per Ca atom and 7.32 wt %. In Table 2, we also listed the recently investigated Ca–carbyne<sup>32</sup> and Ca–graphene results. We see that the Ca–graphyne complex is at least equally efficient as the Ca–carbyne and Ca–graphene systems but with the advantage of not forming the Ca clusters as in the graphene systems. We also note that in the Ca–carbyne system reported in ref 32 a similar advantage exists. In the carbyne system, the strong Ca–carbyne binding energy comes from the interaction of the Ca atom with the single atom C-chain. It seems like the C-chain can deform, which allows four carbon atoms to bind with one Ca atom. In our graphyne case, there is no need for the deformation, and the Ca atom binds to three  $\text{—C}\equiv\text{C—}$  bonds.

We have also tested the graphdiyne system which has already been synthesized.<sup>19</sup> However, due to the large triangle ring in graphdiyne, the Ca atom will fall to a planar position in the graphdiyne ring, and its binding energy to graphdiyne is not as large as the binding energy to graphyne. Besides, such a Ca position will hamper its capability to bind with H<sub>2</sub> molecules. We thus believe the hydrogen storage capability of Ca–graphdiyne is inferior to that of Ca–graphyne.

## CONCLUSION

In summary, using first-principles calculations we found that Ca can bind strongly to the  $s\text{—}p$  and  $s\text{—}p^2$  hybridized carbon graphyne, with its binding energy larger than the Ca cluster cohesive energy. As a result, this solved the biggest obstacle of using Ca decorated fullerene or graphene as a hydrogen storage material: the formation of the Ca cluster. This enhanced binding energy is due to the existence of the extra  $p_x + p_y, \pi/\pi^*$  states in the  $s\text{—}p$  bonded C atoms compared with the Ca–fullerene/graphene systems. The H<sub>2</sub> molecule binding is similar to the Ca–fullerene/graphene system, with a maximum of 6H<sub>2</sub> molecules per Ca atom. The average binding energy is  $\sim 0.2$  eV which is in the desirable range for practical applications. With 6H<sub>2</sub> per Ca atom and two Ca per unit cell, the maximum hydrogen capacity is 9.6 wt %. If 25 °C, 30 atm and 100 °C, 3 atm are used as the absorbing and desorbing conditions, then the practical storage capacity is about 6–7 wt %. Our finding urges the synthesis of the graphyne thin film. The strong Ca–graphyne binding energy shown in this work might also indicate that Ca can be used as a stabilizer for the graphyne structure itself and hence perhaps can be used as a catalyst for graphyne synthesis.

## AUTHOR INFORMATION

### Corresponding Author

\*E-mail: jbli@semi.ac.cn; lwwang@lbl.gov.

## ACKNOWLEDGMENT

J. Li gratefully acknowledges financial support from the “Hundred Talents Program” of the Chinese Academy of Science and National Science Fund for Distinguished Young Scholar (Grant No. 60925016). L.W. Wang’s work at LBNL is supported

by DMS/BES/SC of the U.S. Department of Energy under the contract No. DE-AC02-05CH11231.

## REFERENCES

- (1) Schlappbach, L.; Züttel, A. *Nature (London)* **2001**, *414*, 353.
- (2) Available from, <http://www.eere.energy.gov/hydrogenandfuelcells/mypp/>.
- (3) Li, J.; Furuta, T.; Goto, H.; Ohashi, T.; Fujiwara, Y.; Yip, S. *J. Chem. Phys.* **2003**, *119*, 2376.
- (4) Wang, L.; Yang, R. T. *Catal. Rev.: Sci. Eng.* **2010**, *52*, 411.
- (5) Yildirim, T.; Ciraci, S. *Phys. Rev. Lett.* **2005**, *94*, 175501.
- (6) Zhao, Y. F.; Kim, Y. H.; Dillon, A. C.; Heben, M. J.; Zhang, S. B. *Phys. Rev. Lett.* **2005**, *94*, 155504.
- (7) Reyhani, A.; Mortazavi, S. Z.; Mirershadi, S.; Moshfegh, A. Z.; Parvin, P.; Nozad Golikand, A. *J. Phys. Chem. C* **2011**, *115*, 6994.
- (8) Chen, P.; Wu, X.; Lin, J.; Tan, K. L. *Science* **1999**, *285*, 91.
- (9) Yoon, M.; Yang, S. Y.; Hicke, C.; Wang, E. G.; Geohagan, D.; Zhang, Z. Y. *Phys. Rev. Lett.* **2008**, *100*, 206806.
- (10) Ataca, C.; Aktürk, E.; Ciraci, S. *Phys. Rev. B* **2009**, *79*, 041406(R).
- (11) Lee, H.; Ihm, J.; Cohen, M. L.; Louie, S. G. *Phys. Rev. B* **2009**, *80*, 115412.
- (12) Beheshti, E.; Nojeh, A.; Servati, P. *Carbon* **2011**, *49*, 1561.
- (13) Lee, H.; Ihm, J.; Cohen, M. L.; Louie, S. G. *Nano Lett.* **2010**, *10*, 793.
- (14) Sun, Q.; Wang, Q.; Jena, P.; Kawazoe, Y. *J. Am. Chem. Soc.* **2005**, *127*, 14582.
- (15) Baughman, R. H.; Eckhardt, H.; Kertesz, M. *J. Chem. Phys.* **1987**, *87*, 6687.
- (16) Narita, N.; Nagai, S.; Suzuki, S.; Nakao, K. *Phys. Rev. B* **1998**, *58*, 11009.
- (17) Pan, L. D.; Zhang, L. Z.; Song, B. Q.; Du, S. X.; Gao, H. J. *Appl. Phys. Lett.* **2011**, *98*, 173102.
- (18) Long, M.; Tang, L.; Wang, D.; Li, Y.; Shuai, Z. *ACS Nano* **2011**, *5*, 2593.
- (19) Li, G.; Li, Y.; Liu, H.; Guo, Y.; Li, Y.; Zhu, D. *Chem. Commun.* **2010**, *46*, 3256.
- (20) Kresse, G.; Furthmüller, J. *Phys. Rev. B* **1996**, *54*, 11169 and references therein.
- (21) Blöchl, P. E. *Phys. Rev. B* **1994**, *50*, 17953.
- (22) Perdew, J. P.; Burke, K.; Ernzerhof, M. *Phys. Rev. Lett.* **1996**, *77*, 3865.
- (23) Perdew, J. P.; Burke, K.; Ernzerhof, M. *Phys. Rev. Lett.* **1997**, *78*, 1396.
- (24) Grimme, S. *J. Comput. Chem.* **2006**, *27*, 1787.
- (25) Bučko, T.; Hafner, J.; Lebègue, S.; Ángyán, J. G. *J. Phys. Chem. A* **2010**, *114*, 11814.
- (26) Ceperley, D. M.; Alder, B. J. *Phys. Rev. Lett.* **1980**, *45*, 566.
- (27) Ao, Z. M.; Peeters, F. M. *Phys. Rev. B* **2010**, *81*, 205406.
- (28) Monkhorst, H. J.; Pack, J. D. *Phys. Rev. B* **1976**, *13*, 5188.
- (29) Henkelman, G.; Uberuaga, B. P.; Jónsson, H. *J. Chem. Phys.* **2000**, *113*, 9901.
- (30) Lee, H.; Choi, W. I.; Nguyen, M. C.; Cha, M. H.; Moon, E.; Ihm, J. *Phys. Rev. B* **2007**, *76*, 195110.
- (31) Bhatia, S. K.; Myers, A. L. *Langmuir* **2006**, *22*, 1688.
- (32) Sorokin, P. B.; Lee, H.; Antipina, L.; Singh, A. K.; Yakobson, B. I. *Nano Lett.* **2011**, *11*, 2660.